Dark excitations in monolayer transition metal dichalcogenides

Deilmann, Thorsten; Thygesen, Kristian Sommer

Published in:
Physical Review B

Link to article, DOI:
10.1103/PhysRevB.96.201113

Publication date:
2017

Document Version
Publisher's PDF, also known as Version of record

PHYSICAL REVIEW B **96**, 201113(R) (2017)

Dark excitations in monolayer transition metal dichalcogenides

Thorsten Deilmann[1,*] and Kristian Sommer Thygesen[1,2]

[1]*Center for Atomic-Scale Materials Design (CAMD), Department of Physics, Technical University of Denmark, DK-2800 Kongens Lyngby, Denmark*

[2]*Center for Nanostructured Graphene (CNG), Technical University of Denmark, DK-2800 Kongens Lyngby, Denmark*

(Received 16 July 2017; published 27 November 2017)

Monolayers of transition metal dichalcogenides (TMDCs) possess unique optoelectronic properties, including strongly bound excitons and trions. To date, most studies have focused on optically active excitations, but recent experiments have highlighted the existence of dark states, which are equally important in many respects. Here, we use *ab initio* many-body calculations to unravel the nature of the dark excitations in monolayer $MoSe_2$, MoS_2, WSe_2, and WS_2. Our results show that all these monolayer TMDCs host dark states as their lowest neutral and charged excitations. We further show that dark excitons possess larger binding energies than their bright counterparts while the opposite holds for trions.

DOI: 10.1103/PhysRevB.96.201113

Introduction. The last few years have witnessed an explosion in research on monolayer transition metal dichalcogenides (TMDCs) driven mainly by their unique optical properties [1–8]. In contrast to their bulk counterparts, the monolayer TMDCs possess a direct band gap [9,10] leading to very strong light-matter interactions. Furthermore, the combination of quantum confinement and low dielectric screening in the monolayers leads to a rich excitation spectrum featuring excitons with extremely large binding energies [11]. In addition, charged excitations composed of an exciton with a bound electron/hole, i.e., negative/positive trions, have been observed in experiments on monolayer TMDCs [12–16].

To date, studies of excitations in monolayer TMDCs have mainly focused on the bright, i.e., optically active, states because they are most easily measured. However, basic optical properties such as photoluminescence intensities, exciton decay rates, valley scattering, etc., will depend strongly on the interplay between the bright and dark states in the low-energy part of the spectra [17–19]. In recent experiments by Zhang *et al.* [20] and Molas *et al.* [21], it has been shown that dark excitations can be experimentally probed by applying an in-plane magnetic field. Due to the resulting mixture of dark and bright states, they become visible in photoluminescence. Recent theoretical studies have addressed dark excitons [20,22] using first-principles calculations, however, theory for dark and bright trions has so far exclusively been based on models [23–25]. We note that Feierabend *et al.* [26] proposed further dark excitons with nonzero momenta. Here, we focus on excitation around $\pm K$.

In this Rapid Communication, we revisit the optical excitation spectrum of the monolayer TMDCs MoS_2, $MoSe_2$, WS_2, and WSe_2, paying special attention to the dark excitations. We employ a recently developed method based on first-principles many-body perturbation theory that treats excitons and trions on the same theoretical footing. The electronic properties are calculated in the LDA+GdW approximation [27]. On top of this, we determine the properties of neutral excitons from the Bethe-Salpeter equation (BSE) [28] and the charged trions from a generalization of the BSE to three-particle excitations [29,30].

This Rapid Communication is organized as follows: First, we discuss the energetic position of excitons, and negatively and positively charged trions in freestanding WSe_2. This is followed by a discussion of the role of substrate effects. Finally, we present our results for WS_2, MoS_2, and $MoSe_2$.

The optical absorption spectra of negatively doped and neutral freestanding WSe_2 is shown in Fig. 1(a). The energies of the dark excitations are indicated by the corresponding arrows. We restrict the discussion to the excitations below the first optically active A exciton (see the inset). We find a dark exciton about 80 meV below the A exciton. Figure 1(b) shows the band structure around the K point with the weights of holes and electrons in the exciton wave function indicated. While the hole of the A exciton resides around the valence band (VB) maximum at K (lower red distribution), the electron is found in the second lowest conduction band (CB + 1) (upper red distribution). Instead, the D exciton builds up by contributions from the VB and the lowest CB (blue distribution). The coupling of the exciton to the optical field, i.e., whether the excitation will appear dark or bright, is determined by the spin character of the involved bands. Although in general the spin is not conserved in the presence of strong spin-orbit coupling, this is approximately true in the vicinity of K (and $-K$) and the A and D excitons can thus be characterized as singlet and triplet excitations, respectively.

The energetic splitting of the A and D excitons is determined by three contributions: (i) A single-particle term given by the difference between the CB and CB + 1 (Δ_{so}^{CB}) at K; this amounts to roughly 10 meV. (ii) The (direct) electron-hole interaction which mixes the transitions around K to produce the A and D excitons leads to a 50 meV larger binding energy of the D exciton. This is partially due to the smaller curvature (higher effective mass) of the CB compared to the CB + 1 band [31]. (iii) Finally, the singletlike transitions experience an additional repulsive exchange interaction which lowers the binding energy of the A exciton by ∼20 meV. The three effects add up to the observed difference of 80 meV between D and A. We stress that all of these contributions are of a similar magnitude and must be included for a quantitatively correct analysis.

*thorsten.deilmann@wwu.de

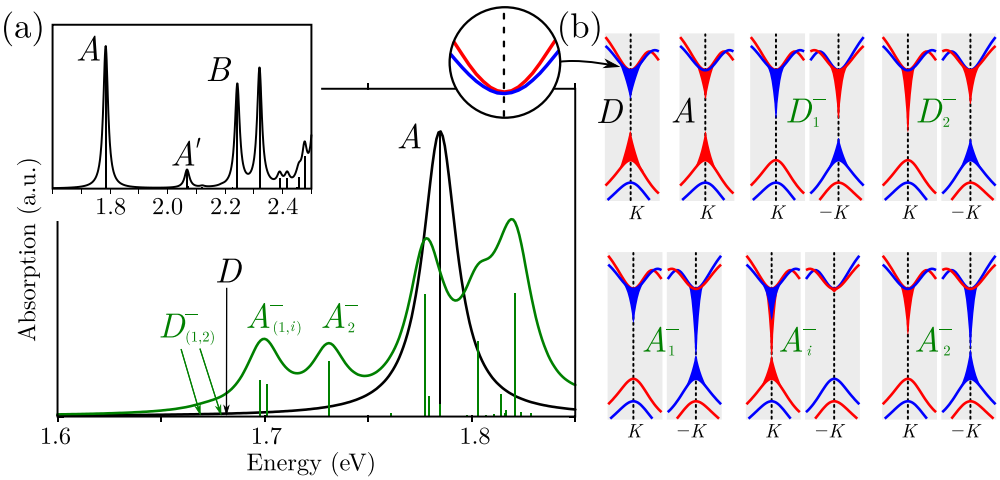

FIG. 1. (a) Optical absorption spectrum of WSe_2 of neutral excitons (black) and negatively charged trions (green) near the lowest possible transitions. The inset shows an overview of the spectrum on a larger scale. We note that we cannot determine the relative weights of excitons and trions as they depend on the doping concentration. The results are shown in the limit of vanishing doping. (b) The contributions of the dark D and bright A excitons, as well as the dark $D^-_{(1,2)}$ and $A^-_{(1,i,2)}$ trions. The red and blue colors denote the spin character of the bands with the contributions from holes and electrons, respectively. The inset next to D is a zoom into the band structure with the CB in blue and CB + 1 in red.

In addition to the neutral excitons, we find five trions for the negatively doped case [Fig. 1(a)]. Two dark trion states $D^-_{(1,2)}$ are located slightly below D, and three optically active trions $A^-_{(1,i,2)}$ are located above D. The dark states originate from the combination of the dark exciton (at $-K$) with an electron in the first or second conduction band at K. On the other hand, the three optically active trions result from combinations of the A exciton (at $-K$) with an additional electron in the first CB at K (A^-_1), or in the second CB at K (A^-_2). Finally, the fifth trion state has all particles located in the same valley (intravalley trion A^-_i).

It is often assumed that a trion can be described as an exciton slightly perturbed by an electron (or hole). Indeed, the energetic ordering of the trions (D^- below D and A^- below A) supports this picture. However, a closer inspection of the probability distribution of electrons and holes in reciprocal space [Fig. 1(b)] shows that the trion is not simply an exciton with an extra electron. First, for all trions we find a more narrow distribution of the electrons than the hole in reciprocal space. This corresponds to a larger extent in real space and is a result of the repulsive electron-electron interaction. Interestingly, part of the "extra" electron in $A^-_{(1,i,2)}$ resides in the same band as the electron of the A exciton. On the other hand, the dark states $D^-_{(1,2)}$ do not show this trend. The relatively complex nature of the trions makes it difficult to predict their energetic ordering. Similar to the case of neutral excitons, the energy of the trions is governed by various factors, including the relative position of the spin-orbit split CB, their curvatures, as well as the strengths of the electron-electron and electron-hole interactions. We postpone the discussion of the relative ordering of dark and bright trions in the MoX_2 and WX_2 TMDCs to the last part of this Rapid Communication.

The excitations discussed above have been proposed previously on the basis of model calculations [24,32]. Employing *ab initio* methods [28,29], we are now able to provide a quantitative prediction of the energy and relative ordering of these excitations, treating dark and bright excitons and trions on the same footing. The lowest state D^-_1 resides at 1.668 eV, i.e., 14 meV below D (trion binding energy). D^-_2 is 11 meV above (conduction band splitting is 10 meV) and is therefore hardly bound. The optically active trions A^-_1 and A^-_i are only slightly split at 1.7 meV ($E_b^{A^-_1} = 60$ meV), while A^-_2 is observed 30 meV above. The larger trion binding energy of bright compared to dark states is a consequence of the modified contributions discussed above. We note in passing that we find further resonant trions around the A exciton [33].

Before comparing our calculations to experiments, we have to account for the effects (band gap renormalization and additional screening resulting in redshifted excitations) due to the substrate on which TMDC monolayers are typically prepared and probed [34]. On SiO_2 we find a redshift of about −25 meV for A and about −15 meV for all other states. Thus we finally obtain a D-A splitting of 70 meV, a trion binding energy of dark states of $E_b^{D^-_1} = 12$ meV, and a trion binding energy of bright states of $E_b^{A^-_1} = 55$ meV.

Experimental binding energies of optically active trions in WSe_2 are typically found to be around 30–40 meV [17]. Also, splittings into two distinct trions (7 meV splitting) have been observed experimentally and have been attributed to the difference between the A^-_1 and A^-_i trions [35]. Zhang *et al.* [20] measure a D-A splitting of 47 meV and trion binding energies of $E^{D^-}_{b,\,expt} = 21$ meV and $E^{A^-}_{b,expt} = 33$ meV, while their GW-BSE calculation predicts 57 meV. In contrast to this, Echeverry *et al.* [22] only predict a value of 16 meV.

Overall, the comparison of our calculations with the available results and particularly the experimental results [20] is good. Most importantly, we reproduce the experimentally observed ordering of D^-, D, A^-, and A excitations. Furthermore, the trend of trion binding energies agrees with experimental findings, i.e., bright trions are more strongly bound than dark trions. On the other hand, our calculated splittings and trion binding energies are slightly larger than observed in experiment. At this point we would like to

stress that there are several factors that complicate the direct comparison between calculations and experiments. First of all, the interpretations and comparisons with experimental spectra are not straightforward. In particular, it is not obvious which states contribute to the different features observed in the measured spectra. Furthermore, environmental screening [34] and finite temperature effects [36] can reduce the trion binding energies. We also note that our calculations are performed for vanishing doping concentration. Stronger doping may affect the band structure and such effects are not accounted for in our calculations. Interestingly, the experimental results of Molas *et al.* [21] for WSe_2 reveal some differences with earlier measurements. In particular, the bright trion is found to have a binding energy of more than 50 meV. In addition, two dark states are found at 47 and 61 meV below the A exciton. On the other hand, the interpretation of these data is slightly more complicated as a large number of states are observed in photoluminescence. In summary, our *ab initio* results are in reasonable agreement with experimental studies and may help to clarify their differences.

In this work we have focused on the trion states that derive from the lowest-lying A and D excitons. However, we have found indications that a similar set of bright and dark trions should be present in front of the B exciton as well as the excited A' exciton, but we postpone the detailed study of these to a later date.

If the sample becomes positively charge (e.g., by applying a gate voltage), the trion spectrum simplifies due to the large spin-orbit induced splitting of the valence bands (in comparison to the conduction band) in all the TMDC monolayers. The large splitting implies that the hole bound to the exciton can only come from the highest-lying valence band. For WSe_2 the VB splitting is 570 meV (480 meV within DFT), compared to the 10 meV splitting in the CB. Consequently, only one dark trion D^+ and one bright A^+ are observed below the A peak in Fig. 2(a). Below the dark D and bright A exciton [identically in Fig. 1(a)], we observe trions with a binding energy $E_b^{D^+} = 14$ meV and $E_b^{A^+} = 29$ meV. While $D^{+/-}$ has a similar excitation energy, it is slightly reduced for the bright excitation A^+ compared to A^- due to the different curvature of the VB. The differences in trion binding energies can again be explained by the difference in the contribution of the holes: Both trions reveal an intervalley character [see contributions in Fig. 2(b)], i.e., no excitation with an intravalley character is present for positive doped TMDCs. The two holes are located around K and $-K$ in the VB maximum, and the electron resides at $-K$ in the CB (CB + 1) for D^+ (A^+).

Comparison with other TMDCs. In the following, we extend the discussion to WS_2, $MoSe_2$, and MoS_2 [37]. As reported previously [22,38], the most significant qualitative difference between these materials with regards to low-lying excitations is the different alignment curvature of the spin-split conduction bands at K [Fig. 3(a)], in particular, whether the conduction band minimum reveals the same spin as the highest valence band. We find values for the spin-orbit induced splitting at the CBM of $\Delta_{so}^{CB} = 41, 15, -10$, and -12 meV for $MoSe_2$, MoS_2, WSe_2, and WS_2, respectively. Due to the inverted character of the conduction bands in MoX_2, it is difficult to predict the energetic ordering of dark and bright excitations. In accordance with previous studies [38–40], we observe that the lowest

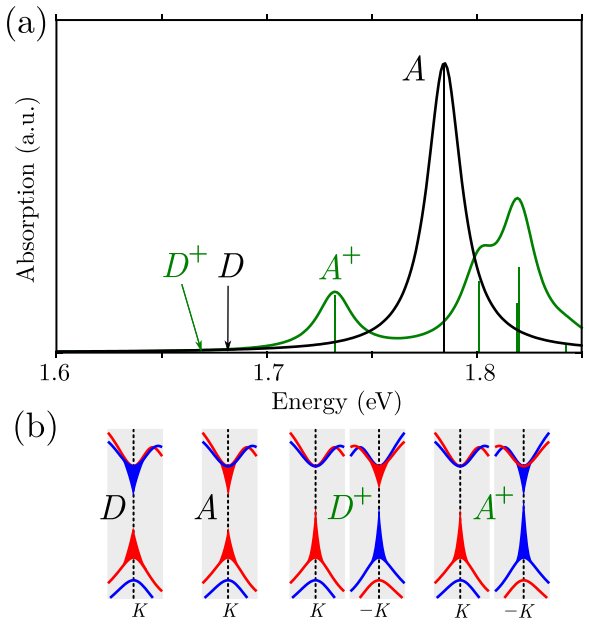

FIG. 2. (a) Optical absorption spectrum of WSe_2 of excitons (black) and positively charged trions (green) near the lowest possible transitions. (b) The contributions of the dark D and bright A exciton, as well as the dark D^+ and A^+ trions. For more details, see the caption of Fig. 1.

exciton is dark in WX_2 (X = S/Se) and MoS_2. However, in contrast to previous results, we also find the dark excitation slightly below the bright ones in $MoSe_2$. This can be traced to the three contributions that determine the position of the dark state (discussed previously for WSe_2). While the difference in single-particle energy as determined by the spin-orbit split CB, Δ_{so}^{CB}, is different from that of WSe_2, the shift due to different effective masses and the reduction of the bright singlet-state binding energy by the exchange interaction are both similar to those found for WSe_2.

The calculated excitation energies of all dark and bright states D, $D^{+/-}$, A, and $A^{+/-}$ are listed in Table I. As explained above, we find dark excitons D below the optically active A in all materials. Due to the inverted character of the CB and CB + 1 for MoS_2 and $MoSe_2$ (by 15 and 41 meV, respectively), the splitting of D and A is, however, decreased

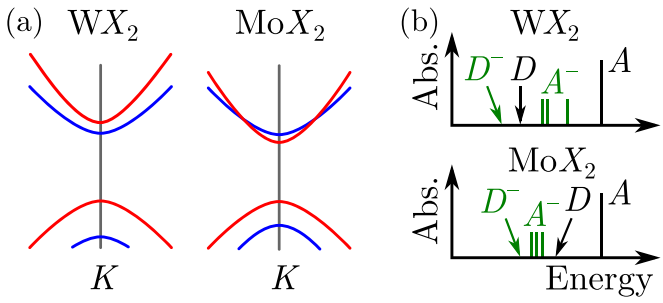

FIG. 3. (a) Schematic band alignment in WX_2 and MoX_2 (X = Se/S) around K. The color denotes the spin character of the bands, i.e., only a transition with spin conservation can be optical active. (b) Sketch of expected absorption spectra including dark excitations.

TABLE I. Exciton energy of the bright state A (in eV), splitting between dark and bright exciton Δ_{DA}, as well as trion binding energies $E_b^{+/-}$ for the given states (in meV). The values in parentheses denote the splitting of the trions with respect to the lowest state. Note that the ordering changes to $A^-_{1,2,i}$ for TMDCs including Mo. All values (in eV) have been obtained by extrapolating to an infinite k-point mesh ($N_k \to \infty$).

TMDC	A	Δ_{DA}	$E_b^{D^-}$	$E_b^{A^-_{1,i,2}}$/ $E_b^{A^-_{1,2,i}}$	$E_b^{D^+}$	$E_b^{A^+}$
WSe_2	1.760	80	15 (11)	65 (3, 33)	15	30
WS_2	2.220	80	10 (12)	60 (1, 26)	15	35
$MoSe_2$	1.770	10	55 (1)	60 (3, 7)	40	55
MoS_2	2.130	25	40 (26)	45 (2, 5)	25	40

in these materials. Furthermore, we also find bound dark trion states $D^-_{(1,2)}$, which turn out to have the lowest excitation energies (of all the investigated quasiparticles). We observe the same characteristic three trion states $A^-_{(1,2,i)}$ (as already discussed for WSe_2) in all the materials. As a general trend, the energy of intervalley trions ($D^-_{(1,2)}$ and $A^-_{(1,2)}$) are always lower if the additional electron resides in the lower band (CB) in the other valley, i.e., D_2^- and A_2^- are shifted to higher energies. Second, the intravalley trion A_i^- resides slightly above A_1^- (less than 10 meV) in which the electrons reside in the same bands with the additional electron in different valleys. Due the inverted character of the conduction bands including Mo, the splitting of $A^-_{(1,i,2)}$ is decreased and the order of the three states changes from $A^-_{(1,i,2)}$ to $A^-_{(1,2,i)}$.

As a consequence of the reduced D-A splitting in the MoX_2 monolayers, the ordering of the excitations change. Specifically, for MoS_2 and $MoSe_2$, we find (in order of increasing energy) D^-, A^-, D, and A as sketched in Fig. 3(b). For positive doping we find that the excitations reorders in the same manner, i.e., we find the A^+ trion below the corresponding D excitons for TMDCs including Mo.

Finally, we qualitatively discuss the possibility of observing the different excitations in photoluminescence experiments [21]. For example, for the formation of a negative trion, an exciton and an extra electron are required. Assuming a Boltzmann distribution of electron states (e.g., due to doping by a substrate), the occupation of higher-lying bands will be exponentially suppressed. In particular, for $MoSe_2$ with the largest CB splitting of 41 meV, we expect the formation of an A trion to be much more likely than the formation of D trions. The lower weight and the small splitting between dark and bright states may prohibit the observation in experiment. In contrast to this, TMDCs including W will show an inverted trend, i.e., the dark states should be more likely than bright states. However, the weight of dark states in photoluminescence will also depend on the mixing to bright states via the applied in-plane magnetic field [20,21].

In summary, we have presented an *ab initio* study of the lowest-lying bright and dark excitations in monolayer $MoSe_2$, MoS_2, WSe_2, and WS_2. Using a recently developed generalization of the Bethe-Salpeter equation to three-particle states we were able to describe excitons and trions on the same theoretical footing. This allowed us to obtain quantitative results for the excitation energy, binding energy, and composition of the A, D, $A^{+/-}$, and $D^{+/-}$ excitations. Our results show that the lowest-lying excitons and trions are dark in all materials. The relative ordering of the excitations was found to differ for W- and Mo-based TMDCs. In particular, the dark exciton (D) lies above the bright trions in MoX_2 while it lies below in WX_2. In accordance with experiment, we observe that dark trions are weaker bound than bright states. Our results provide a useful reference for the analysis and interpretation of experimental optical spectra of monolayer TMDCs. Furthermore, they highlight the importance of dark states and indicate that these could play an important role for the carrier dynamics in optically excited TMDCs.

Acknowledgments. T.D. acknowledges financial support from the Villum Foundation. The Center for Nanostructured (CNG) is sponsored by the Danish Research Foundation, Project No. DNRF103.

[1] K. F. Mak, K. He, J. Shan, and T. F. Heinz, Control of valley polarization in monolayer MoS_2 by optical helicity, Nat. Nanotechnol. **7**, 494 (2012).

[2] G. Sallen, L. Bouet, X. Marie, G. Wang, C. R. Zhu, W. P. Han, Y. Lu, P. H. Tan, T. Amand, B. L. Liu, and B. Urbaszek, Robust optical emission polarization in MoS_2 monolayers through selective valley excitation, Phys. Rev. B **86**, 081301(R) (2012).

[3] H. Zeng, J. Dai, W. Yao, D. Xiao, and X. Cui, Valley polarization in MoS_2 monolayers by optical pumping, Nat. Nanotechnol. **7**, 490 (2012).

[4] T. Cao, G. Wang, W. Han, H. Ye, C. Zhu, J. Shi, Q. Niu, P. Tan, E. Wang, B. Liu, and J. Feng, Valley-selective circular dichroism of monolayer molybdenum disulphide, Nat. Commun. **3**, 887 (2012).

[5] D. Xiao, G.-B. Liu, W. Feng, X. Xu, and W. Yao, Coupled Spin and Valley Physics in Monolayers of MoS_2 and Other Group-VI Dichalcogenides, Phys. Rev. Lett. **108**, 196802 (2012).

[6] Z. Yin, H. Li, H. Li, L. Jiang, Y. Shi, Y. Sun, G. Lu, Q. Zhang, X. Chen, and H. Zhang, Single-layer MoS_2 phototransistors, ACS Nano **6**, 74 (2012).

[7] A. Srivastava, M. Sidler, A. V. Allain, D. S. Lembke, A. Kis, and A. Imamoğlu, Optically active quantum dots in monolayer WSe_2, Nat. Nanotechnol. **10**, 491 (2015).

[8] M. Koperski, K. Nogajewski, A. Arora, V. Cherkez, P. Mallet, J.-Y. Veuillen, J. Marcus, P. Kossacki, and M. Potemski, Single photon emitters in exfoliated WSe_2 structures, Nat. Nanotechnol. **10**, 503 (2015).

[9] K. F. Mak, C. Lee, J. Hone, J. Shan, and T. F. Heinz, Atomically Thin MoS_2: A New Direct-Gap Semiconductor, Phys. Rev. Lett. **105**, 136805 (2010).

[10] A. Splendiani, L. Sun, Y. Zhang, T. Li, J. Kim, C.-Y. Chim, G. Galli, and F. Wang, Emerging photoluminescence in monolayer MoS_2, Nano Lett. **10**, 1271 (2010).

[11] K. S. Thygesen, Calculating excitons, plasmons, and quasiparticles in 2D materials and van der Waals heterostructures, 2D Mater. **4**, 022004 (2017).

[12] K. F. Mak, K. He, C. Lee, G. H. Lee, J. Hone, T. F. Heinz, and J. Shan, Tightly bound trions in monolayer MoS_2, Nat. Mater. **12**, 207 (2013).

[13] J. S. Ross, S. Wu, H. Yu, N. J. Ghimire, A. M. Jones, G. Aivazian, J. Yan, D. G. Mandrus, D. Xiao, W. Yao, and X. Xu, Electrical control of neutral and charged excitons in a monolayer semiconductor, Nat. Commun. **4**, 1474 (2013).

[14] C. Zhang, H. Wang, W. Chan, C. Manolatou, and F. Rana, Absorption of light by excitons and trions in monolayers of metal dichalcogenide MoS_2: Experiments and theory, Phys. Rev. B **89**, 205436 (2014).

[15] S. Mouri, Y. Miyauchi, and K. Matsuda, Tunable photoluminescence of monolayer MoS_2 via chemical doping, Nano Lett. **13**, 5944 (2013).

[16] A. Singh, G. Moody, K. Tran, M. E. Scott, V. Overbeck, G. Berghäuser, J. Schaibley, E. J. Seifert, D. Pleskot, N. M. Gabor, J. Yan, D. G. Mandrus, M. Richter, E. Malic, X. Xu, and X. Li, Trion formation dynamics in monolayer transition metal dichalcogenides, Phys. Rev. B **93**, 041401(R) (2016).

[17] A. M. Jones, H. Yu, N. J. Ghimire, S. Wu, G. Aivazian, J. S. Ross, B. Zhao, J. Yan, D. G. Mandrus, D. Xiao, W. Yao, and X. Xu, Optical generation of excitonic valley coherence in monolayer WSe_2, Nat. Nanotechnol. **8**, 634 (2013).

[18] A. Singh, K. Tran, M. Kolarczik, J. Seifert, Y. Wang, K. Hao, D. Pleskot, N. M. Gabor, S. Helmrich, N. Owschimikow, U. Woggon, and X. Li, Long-Lived Valley Polarization of Intravalley Trions in Monolayer WSe_2, Phys. Rev. Lett. **117**, 257402 (2016).

[19] F. Volmer, S. Pissinger, M. Ersfeld, S. Kuhlen, C. Stampfer, and B. Beschoten, Intervalley dark trion states with spin lifetimes of 150 ns in WSe_2, Phys. Rev. B **95**, 235408 (2017).

[20] X.-X. Zhang, T. Cao, Z. Lu, Y.-C. Lin, F. Zhang, Y. Wang, Z. Li, J. C. Hone, J. A. Robinson, D. Smirnov, S. G. Louie, and T. F. Heinz, Magnetic brightening and control of dark excitons in monolayer WSe2, Nat. Nanotechnol. **12**, 883 (2017).

[21] M. R. Molas, C. Faugeras, A. O. Slobodeniuk, K. Nogajewski, M. Bartos, D. M. Basko, and M. Potemski, Brightening of dark excitons in monolayers of semiconducting transition metal dichalcogenides, 2D Mater. **4**, 021003 (2017).

[22] J. P. Echeverry, B. Urbaszek, T. Amand, X. Marie, and I. C. Gerber, Splitting between bright and dark excitons in transition metal dichalcogenide monolayers, Phys. Rev. B **93**, 121107(R) (2016).

[23] T. C. Berkelbach, M. S. Hybertsen, and D. R. Reichman, Theory of neutral and charged excitons in monolayer transition metal dichalcogenides, Phys. Rev. B **88**, 045318 (2013).

[24] H. Yu, X. Cui, X. Xu, and W. Yao, Valley excitons in two-dimensional semiconductors, Natl. Sci. Rev. **2**, 57 (2015).

[25] M. Danovich, V. Zólyomi, and V. I. Fal'ko, Dark trions and biexcitons in WS_2 and WSe_2 made bright by *e-e* scattering, Sci. Rep. **7**, 45998 (2017).

[26] M. Feierabend, G. Berghäuser, A. Knorr, and E. Malic, Proposal for dark exciton based chemical sensors, Nat. Commun. **8**, 14776 (2017).

[27] M. Rohlfing, Electronic excitations from a perturbative LDA+GdW approach, Phys. Rev. B **82**, 205127 (2010).

[28] G. Strinati, Dynamical Shift and Broadening of Core Excitons in Semiconductors, Phys. Rev. Lett. **49**, 1519 (1982).

[29] T. Deilmann, M. Drüppel, and M. Rohlfing, Three-Particle Correlation from a Many-Body Perspective: Trions in a Carbon Nanotube, Phys. Rev. Lett. **116**, 196804 (2016).

[30] We note that the absolute precision of the band structure and excitations cannot be expected to be better than 0.1 eV, however, the relative position of the different excitations is expected to be smaller than 10 meV. See Supplemental Material at http://link.aps.org/supplemental/10.1103/PhysRevB.96.201113 for a discussion of the methods and further numerical details.

[31] The change of the exciton binding energy for different effective masses can be understood in a simple two-band model [41].

[32] E. Courtade, M. Semina, M. Manca, M. M. Glazov, C. Robert, F. Cadiz, G. Wang, T. Taniguchi, K. Watanabe, M. Pierre, W. Escoffier, E. L. Ivchenko, P. Renucci, X. Marie, T. Amand, and B. Urbaszek, Charged excitons in monolayer WSe_2: Experiment and theory, Phys. Rev. B **96**, 085302 (2017).

[33] While the five discussed trions are well converged (and extrapolated for any infinite k mesh), resonant trions are computationally much more demanding.

[34] M. Drüppel, T. Deilmann, P. Krüger, and M. Rohlfing, Diversity of trion states and substrate effects in the optical properties of an MoS_2 monolayer, Nat. Commun. (to be published).

[35] A. M. Jones, H. Yu, J. R. Schaibley, J. Yan, D. G. Mandrus, T. Taniguchi, K. Watanabe, H. Dery, W. Yao, and X. Xu, Excitonic luminescence upconversion in a two-dimensional semiconductor, Nat. Phys. **12**, 323 (2015).

[36] J. W. Christopher, B. B. Goldberg, and A. K. Swan, Long tailed trions in monolayer MoS_2: Temperature dependent asymmetry and red-shift of trion photoluminescence spectra, Sci. Rep. **7**, 14062 (2017).

[37] For MoS_2, also see Ref. [34].

[38] M. Koperski, M. R. Molas, A. Arora, K. Nogajewski, A. O. Slobodeniuk, C. Faugeras, and M. Potemski, Optical properties of atomically thin transition metal dichalcogenides: Observations and puzzles, Nanophotonics **6**, 1289 (2017).

[39] D. Y. Qiu, T. Cao, and S. G. Louie, Nonanalyticity, Valley Quantum Phases, and Lightlike Exciton Dispersion in Monolayer Transition Metal Dichalcogenides: Theory and First-Principles Calculations, Phys. Rev. Lett. **115**, 176801 (2015).

[40] We note that while Qiu *et al.* [39] observe a dark state about 40 meV below the bright one, Echeverry *et al.* [22] observe a vanishing difference for MoS_2.

[41] T. Olsen, S. Latini, F. Rasmussen, and K. S. Thygesen, Simple Screened Hydrogen Model of Excitons in Two-Dimensional Materials, Phys. Rev. Lett. **116**, 056401 (2016).